

Dynamical Scenarios of Changes in Asymmetric Relationships Over Time (1)

Naohito CHINO*

Abstract

This paper is the first part of the revised version of my paper presented elsewhere (Chino, 2017). In this paper we propose a recent version of a set of complex difference equation models which describes changes in asymmetric relationships among objects over time. Typical examples of these objects may be citation frequencies in scientific publications, amounts of trade among nations, connections among neurons, and so on. Supposing that such an asymmetric relational data matrix or a weighted digraph is observed in an instant of time, we first apply the Chino-Shiraiwa theorem to the matrix and embed objects in a (complex) Hilbert space. Then we shall apply our recent version of a set of general complex difference equation models to the initial configuration of objects embedded in the Hilbert space. As a result, we have various possible theoretical scenarios of the trajectories of objects in this space. We show some of the possible scenarios of the linear difference equation models in the special cases when the number of objects are two and three. In a companion paper to be published soon, we show various possible scenarios of the nonlinear difference equation models.

Keywords: complex difference equation, Hilbert space, Chino-Shiraiwa theorem, dynamic weighted digraph, chaos, trade imbalance, neural network

1. Introduction

The formation of group structures and their changes over time within complex systems are ubiquitous in nature, and have a self-organizing property in most cases. Typical examples of these networks may be citation frequencies in scientific publications (i.e., Barabási & Albert, 1999; Chino, 1978), amounts of trade among nations (i.e., Chino, 1978), and connections among neurons (i.e., Aizenberg et al., 1971, 2000; Hirose, 1992; Suksmono & Hirose, 2005).

One method to analyze such structures is to use a graph theoretic approach. Watts and Strogatz (1998) proposed the *small world model*, which is characterized by the property that two nodes (vertices) can be connected with a path (edges) of a few links only. Barabási and Albert (1999) found that many large networks have a common property in which the distribution function of vertex connectivities obeys a *scale-free power law*.

Although graph theory is promising, it has a fundamental shortfall in that each path is in most cases assumed to be bi-

nary. It might be desirable to consider some models which describe changes in strengths of interaction between group members, i.e., changes in weights of directed graph (digraph), since in actual networks strengths of interaction are frequently continuous. One method to do such a job is to utilize dynamical system theories.

For example, McCann et al. (1998) proposed an interesting *nonlinear differential equation model* as a food-web model, in which they considered food-webs composed of three or four species, one being the top predator, another being a resource species, and the others being one or two consumer species. They examined the effects of interaction strengths on changes in densities of species over time. Results indicated that chaotic behaviors occur when the interaction strengths as bifurcation parameters of the system vary as time proceeds.

Chesson and Warner (1981) proposed a lottery model which is described by a set of *nonlinear difference equations*. This model explains a certain coexistence phenomenon of species. However, these models merely deal with

*Department of Psychology, Faculty of Psychological and Physical Science, Aichi Gakuin University.

Requests for reprints should be sent to: chino@dpc.agu.ac.jp

This is the first part of the revised version of my paper titled “Dynamical scenarios of changes in asymmetric relationships on a Hilbert space” presented at the 45th annual meeting of the Behaviormetric Society of Japan, Shizuoka, Japan.

changes in numbers or density of species. Moreover, most of the network models discussed above assume that the state space of the system is *real*, except for the *complex* neural network models.

In this paper, we shall discuss various possible dynamical scenarios of a family of difference equation models. In these models, the state space is assumed to be *finite-dimensional Hilbert space*, given an asymmetric relational data matrix observed at a particular instant in time. Assumption of the Hilbert space is an algebraic consequence of the application of Chino and Shiraiwa theorem (Chino & Shiraiwa, 1993) to the asymmetric matrix.

The earlier primitive model (Chino, 2000, 2002, 2006, 2014, 2015) is written as the following set of equations:

$$\mathbf{z}_{j,n+1} = \mathbf{z}_{j,n} + \sum_{m=1}^q \sum_{k \neq j}^N \mathbf{D}_{jk}^{(m)} \mathbf{f}^{(m)}(\mathbf{z}_{j,n} - \mathbf{z}_{k,n}), \quad (1)$$

$$j = 1, 2, \dots, N,$$

$$\mathbf{f}^{(m)}(\mathbf{z}_{j,n} - \mathbf{z}_{k,n}) = \left((z_{j,n}^{(1)} - z_{k,n}^{(1)})^m, (z_{j,n}^{(2)} - z_{k,n}^{(2)})^m, \dots, (z_{j,n}^{(p)} - z_{k,n}^{(p)})^m \right)^t, \quad (2)$$

and

$$\mathbf{D}_{jk,n}^{(m)} = \text{diag} \left(w_{jk,n}^{(1,m)}, w_{jk,n}^{(2,m)}, \dots, w_{jk,n}^{(p,m)} \right). \quad (3)$$

$$w_{jk,n}^{(l,m)} = a_{j,n}^{(l,m)} r_{j,n}^{(l,m)} r_{k,n}^{(l,m)} \sin \left(\theta_{k,n}^{(l,m)} - \theta_{j,n}^{(l,m)} \right), \quad (4)$$

$$l=1, 2, \dots, p, \quad m=1, 2, \dots, q.$$

Here, $\mathbf{z}_{j,n}$ denotes the coordinate vector of member j at time n in a p -dimensional Hilbert space or an indefinite metric space. Moreover, m denotes the degree of the vector function, $\mathbf{f}^{(m)}(\mathbf{z}_{j,n} - \mathbf{z}_{k,n})$, which is assumed to have the maximum value q . This model is very general and might enable us to describe various possible changes in asymmetric relationships among members over time.

However, recently we have found that Eq. (4) is *too restrictive* to model various complex phenomena. Moreover, we have recently realized that there exists an essential defect in Eq. (4). That is, with this equation, the above difference equation is not *holomorphic*. For these reasons, we have recently dropped Eq. (4) from our model.

As a result, the current version of our model is composed of a revised version of Eq. (1), Eq. (2), and Eq. (3). It should be noticed that $w_{jk,n}^{(1,m)}, w_{jk,n}^{(2,m)}, \dots, w_{jk,n}^{(p,m)}$ in Eq. (3) are *complex constants* in this case. Thus, we shall drop the subscript, n , in Eq. (3). Then, the revised version of Eq. (1) is written as,

$$\mathbf{z}_{j,n+1} = \mathbf{z}_{j,n} + \sum_{m=1}^q \sum_{k \neq j}^N \mathbf{D}_{jk}^{(m)} \mathbf{f}^{(m)}(\mathbf{z}_{j,n} - \mathbf{z}_{k,n}) + \mathbf{g}(\mathbf{u}_{j,n}) + \mathbf{z}_0, \quad j = 1, 2, \dots, N, \quad (5)$$

where $\mathbf{g}(\mathbf{u}_{j,n})$ is a control (e.g., Elaydi, 1999; Ott et al., 1990), and \mathbf{z}_0 is a complex constant vector. We may absorb \mathbf{z}_0 into $\mathbf{g}(\mathbf{u}_{j,n})$ in Eq. (5). In this case Eq. (5) can be further revised as

$$\mathbf{z}_{j,n+1} = \mathbf{z}_{j,n} + \sum_{m=1}^q \sum_{k \neq j}^N \mathbf{D}_{jk}^{(m)} \mathbf{f}^{(m)}(\mathbf{z}_{j,n} - \mathbf{z}_{k,n}) + \mathbf{g}(\mathbf{u}_{j,n}, \mathbf{z}_0), \quad j = 1, 2, \dots, N. \quad (6)$$

This means that we consider the complex constant, \mathbf{z}_0 , as a control factor.

2. Introduction to an elementary theory of dynamic weighted digraph

To facilitate the understanding of the current set of difference equation models defined in the previous section and the motivation of this study, we shall show two sets of data. One set of data is the weighted digraph among four countries, Japan, Amerika, China, and Russia in 2015 (Asahi Newspaper, 2015). The corresponding asymmetric relational data matrix is shown in Table 1.

Table 1. Asymmetric relational data matrix among four countries, Japan, Amerika, China, and Russia in 2015, which was reproduced from the figure appeared in elsewhere (Asahi Newspaper, 2015).

	J. Japan	A. America	C. China	R. Russia
J. Japan	43,480	1,382	1,200	55
A. America	736	189,592	1,161	71
C. China	1,764	4,832	119,684	348
R. Russia	173	146	333	13,755

Application of HFM (Chino & Shiraiwa, 1993) to the log transformed trade data revealed a *4-dimensional Hilbert space structure*, since the eigenvalues of the Hermitian matrix computed from the above asymmetric matrix were 29.9714, 6.1145, 4.4377, and 3.5309. Here, we shall approximate this structure by a *one-dimensional Hilbert space structure* (i.e., the complex plane) associated with the largest eigenvalue. Figure 1 shows the configuration of the four nations corresponding to the largest eigenvalue on the complex plane.

Then, in what manner does the configuration of these nations change theoretically as time proceeds, through the interactions among nations? Our complex difference equation models predict various scenarios of changes in the configuration in terms of the trajectories of our models for these nations. Moreover, how can we change the configuration of nations, or paraphrase it to say, how can we control the trade imbalances revealed by the configuration of nations?

One possible theoretical scenario is shown in Figure 2.

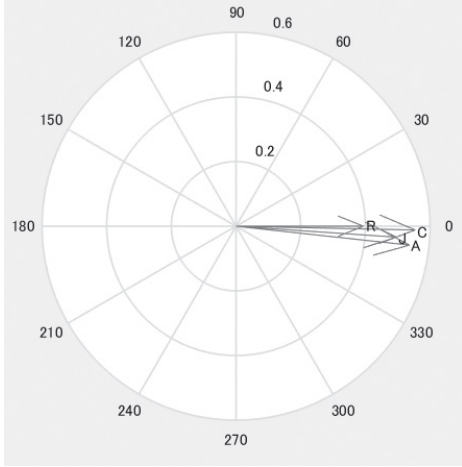


Fig. 1. Configuration of the four nations associated with the largest eigenvalue of the Hermitian matrix corresponding to the asymmetric trade data matrix.

The unit length of the imaginary axis (i.e., the vertical axis) is enlarged compared with that of Figure 1. In this figure, the points labelled A_1 , C_1 , J_1 , and R_1 denote the initial points of America, China, Japan, and Russia, respectively, in the complex plane. After the 800 iterations of a linear difference equation model, these four points converge almost to the point labelled $JACR_{800}$. According to HFM, this means that the trade imbalance among four nations dissolves as time proceeds.

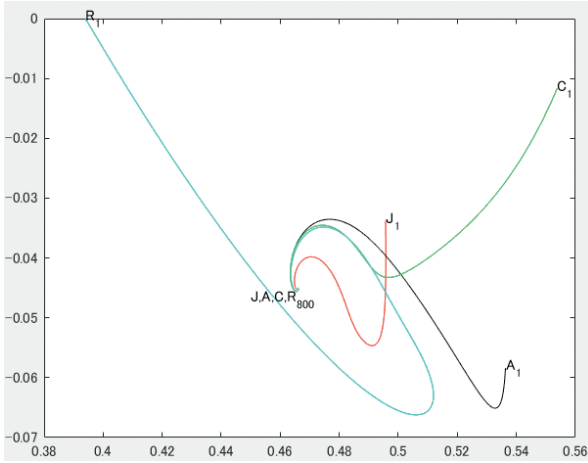


Fig. 2. Trajectories of the four nations, Japan, Amerika, China, and Russia after 800 iterations of Model IV of the complex linear difference equation model, $\mathbf{z}_{n+1} = \mathbf{A}_4 \mathbf{z}_n$ where \mathbf{A}_4 is the weight matrix of order 4 which is similar to \mathbf{A}_3 in Eq. (7), and its weights are $\alpha_{jk} = -0.01(1 - i)$, $\alpha_{jm} = \alpha_{km} = \alpha_{jl} = \alpha_{kl} = \alpha_{lm} = 0.01(1 - i)$, $\alpha_{kj} = \alpha_{mj} = \alpha_{mk} = \alpha_{lj} = \alpha_{lk} = \alpha_{ml} = -0.02(1 - i)$. In this case, eigenvalues of \mathbf{A}_4 are 1.0, 0.9950, 0.9901, and 0.9754.

The other set of data is the estimated pass diagram among three voxels, V1 (primary visual cortex), V5 (middle temporal area), and SPC (superior parietal cortex), which was presented by Takane (2015). We modified the original pass diagram in such a way that it includes only the *weighted digraph among three voxels*. Table 2 shows the corresponding asymmetric connection matrix among three voxels.

Table 2. An asymmetric connection matrix among three voxels corresponding to the digraph which is a modified version of that analyzed by Takane (2015).

	V1	V5	SPC
V1	0.329	0.601	0.335
V5	0.347	-0.044	0.404
SPC	0.146	0.307	0.052

HFM applied to this set of data tells us that the above asymmetric connections have an *indefinite metric structure*, since the eigenvalues of the Hermitian matrix computed from the above asymmetric matrix are 0.8811, -0.0972 , and -0.4469 . Here, we shall approximate this structure by a one-dimensional Hilbert space structure associated with the largest eigenvalue. Figure 3 shows the configuration of the three voxels corresponding to the largest eigenvalue.

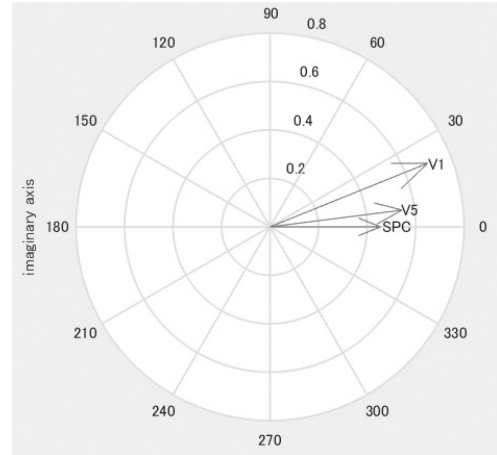


Fig. 3. Configuration of the three voxel, V1, V5, and SPC associated with the largest eigenvalue of the Hermitian matrix corresponding to the asymmetric connection matrix, elements of which are the pass coefficients by Takane (2015).

Here, let us suppose that we have observed the above configuration of the three voxels at an instant of time. Then, in what manner does the configuration of these voxels change theoretically as time proceeds through the interactions among voxels?

Our complex difference equation models predict various scenarios of changes in the configuration in terms of the trajectories of our models for these voxels. In this case, we used a *quadratic* difference equation model described by Eq. (15) defined in the next section. One reason why we choose such a nonlinear difference equation model for analyzing the set of data is that various chaotic behaviors have been found elsewhere in the neural network literature (i.e., Aihara et al., 1998; Babloyantz & Destexhe, 1986; Dafillis et al., 2013; Korn & Fauke, 2003; Mees et al., 1992; Pereda et al., 1998). Another reason is that linear models are unable to describe chaotic behaviors.

Figures 4 to 5 show some of the simulation results. Coefficients α_{jk} 's in this simulation are set equal to: $\alpha_{jk}^{(1)} = \alpha_{jk}^{(2)} = 0.01$, $\alpha_{jl}^{(1)} = \alpha_{jl}^{(2)} = 0.01(-0.5 - 0.5i)$, $\alpha_{kl}^{(1)} = \alpha_{kl}^{(2)}$, $\alpha_{kl}^{(1)} = \alpha_{kl}^{(2)} = 0.01(1.5375 - 0.9564i)$, $\alpha_{kj}^{(1)} = -0.01$, $\alpha_{kj}^{(2)} = \alpha_{jk}^{(2)}$, $\alpha_{lj}^{(1)} = \alpha_{jl}^{(1)}$, $\alpha_{lj}^{(2)} = \alpha_{jl}^{(2)}$, $\alpha_{lk}^{(1)} = \alpha_{kl}^{(1)}$, $\alpha_{lk}^{(2)} = \alpha_{kl}^{(2)}$, where α 's are coefficients of a quadratic system described by Eq. (15).

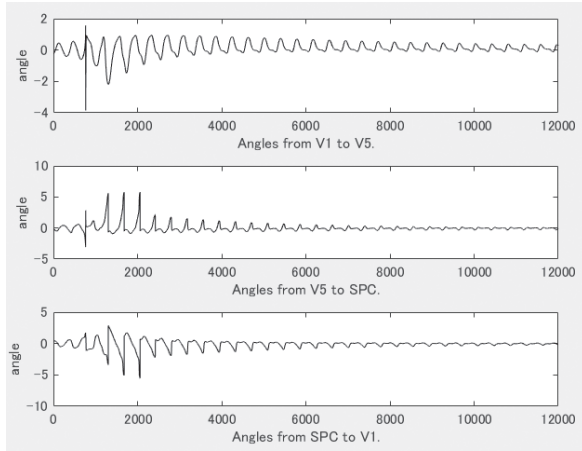


Fig. 4. Changes in angles between voxels over time in the special case when α 's are special values.

Figure 4 draws the node-to-node responses of the three voxels during the 12,000 iterations by a nonlinear system described by Eq. (15). It is apparent that the node-to-node responses behave as if they were the output from a damped oscillator after about 2000 iterations.

Figure 5 draws the trajectories of the three voxels, V1, V5, and SPC on the complex plane after 12,000 iterations. At an initial stage, trajectories of these voxels are all unstable and run about in a wide region, but they gradually begin to diverge, rotating on different cylinder-like spheres.

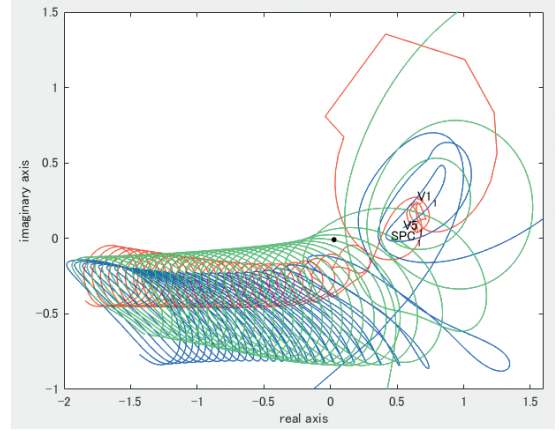


Fig. 5. Trajectories of the three voxels, V1, V5, and SPC on the complex plane in the special case when α 's are special values.

3. Dynamical scenarios of changes in asymmetric relationships in complex difference models

The difference equation models which we discuss in this section are some special cases of the general nonlinear difference equation model composed of Eqs. (5), (2), and (3), which is called “Model IV” in Chino (2016):

First, we assume the special case when $m=1$, $p=1$, $\mathbf{g}(\mathbf{u}_{j,n})=\mathbf{0}$, and $\mathbf{z}_0=\mathbf{0}$. If we further assume $N=2$, this case becomes a *dyadic* linear difference equation model, i.e.,

$$\begin{cases} z_{j,n+1} = z_{jn} + \alpha_{jk}(z_{jn} - z_{kn}) \\ z_{k,n+1} = z_{kn} + \alpha_{kj}(z_{kn} - z_{jn}) \end{cases} \quad (7)$$

and if we assume $N=3$, it becomes a *triadic* linear difference equation model, i.e.,

$$\begin{cases} z_{j,n+1} = z_{jn} + \alpha_{jk}(z_{jn} - z_{kn}) + \alpha_{jl}(z_{jn} - z_{ln}) \\ z_{k,n+1} = z_{kn} + \alpha_{kl}(z_{kn} - z_{ln}) + \alpha_{kj}(z_{kn} - z_{jn}) \\ z_{l,n+1} = z_{ln} + \alpha_{lj}(z_{ln} - z_{jn}) + \alpha_{lk}(z_{ln} - z_{kn}) \end{cases} \quad (8)$$

and so on.

If we use the vector notation, Eqs. (7) and (8) can be written, respectively, as

$$\mathbf{z}_{n+1} = \mathbf{A}_2 \mathbf{z}_n, \quad \text{where } \mathbf{A}_2 = \begin{pmatrix} 1 + \alpha_{jk} & -\alpha_{jk} \\ -\alpha_{kj} & 1 + \alpha_{kj} \end{pmatrix}, \quad (9)$$

and

$$\mathbf{z}_{n+1} = \mathbf{A}_3 \mathbf{z}_n, \quad \text{where } \mathbf{A}_3 = \begin{pmatrix} 1 + \alpha_{jk} + \alpha_{jl} & -\alpha_{jk} & -\alpha_{jl} \\ -\alpha_{kj} & 1 + \alpha_{kl} + \alpha_{kj} & -\alpha_{kl} \\ -\alpha_{lj} & -\alpha_{lk} & 1 + \alpha_{lj} + \alpha_{lk} \end{pmatrix}. \quad (10)$$

Eqs. (9) and (10) are linear difference equations, and can be solved, for example, by using the famous Putzer algorithm

(Putzer, 1966). Dynamical scenarios of the solution curves can be examined by considering the *eigenvalues* of matrices, A_2 , A_3 , and so on. It is evident that these matrices have at least one eigenvalue of size 1.

In the dyadic case, dynamical scenarios of the solution curve have three patterns depending on the absolute value of the eigenvalue, $1 + \alpha_{jk} + \alpha_{kj}$, as follows:

$$\begin{cases} \text{diverge,} & \text{if } |1 + \alpha_{jk} + \alpha_{kj}| > 1 \\ \text{diverge on two lines,} & \text{if } |1 + \alpha_{jk} + \alpha_{kj}| = 1 \\ \text{converge,} & \text{if } |1 + \alpha_{jk} + \alpha_{kj}| < 1 \end{cases} \quad (11)$$

If we add a control term defined in Eq. (5), this becomes a dyadic difference equation model with a control term. If we assume, for example, that $\mathbf{g}(\mathbf{u}_{j,n}) = (0.01ni, 0.02)^t$, Eq. (7) is written as

$$\begin{cases} z_{j,n+1} = z_{jn} + \alpha_{jk}(z_{jn} - z_{kn}) + 0.01ni, \\ z_{k,n+1} = z_{kn} + \alpha_{kj}(z_{kn} - z_{jn}) + 0.02, \end{cases} \quad (12)$$

where $i^2 = -1$. This type of system is easily solved algebraically. We shall compare its trajectory with those of the systems described by Eq. (7) later.

Finally, we consider difference equation models with quadratic terms. If we assume the special case when $N=2$, $m=2$, $p=1$, $\mathbf{g}(\mathbf{u}_{j,n})=\mathbf{0}$, and $\mathbf{z}_0=\mathbf{0}$ in Eq. (5), then we have

$$\begin{cases} z_{j,n+1} = z_{jn} + \alpha_{jk}^{(1)}(z_{jn} - z_{kn}) + \alpha_{jk}^{(2)}(z_{jn} - z_{kn})^2, \\ z_{k,n+1} = z_{kn} + \alpha_{kj}^{(1)}(z_{kn} - z_{jn}) + \alpha_{kj}^{(2)}(z_{kn} - z_{jn})^2. \end{cases} \quad (13)$$

This type of system has a very desirable property in that we can utilize the heritage of the theory of the complex dynamical system developed in mathematics directly in classifying its trajectories. In fact, defining a new variable, $u_{jkn} = z_{jn} - z_{kn}$, and transforming it linearly, we have a new system

$$\begin{aligned} Z_{jk,n+1} &= Z_{jk,n}^2 + \gamma_{jk}^{(1)}, \\ \text{where } \gamma_{jk}^{(1)} &= \frac{1}{2}\beta_{jk}^{(1)} - \frac{1}{4}[\beta_{jk}^{(1)}]^2, \end{aligned} \quad (14)$$

and $\beta_{jk}^{(1)} = 1 + \alpha_{jk}^{(1)} + \alpha_{kj}^{(1)}$ (K. Shiraiwa, personal communication, April 25, 2014). Depending on the value of $\gamma_{jk}^{(1)}$, we have the *Mandelbrot set*. It is interesting to note that $\beta_{jk}^{(1)}$ which determines the value of $\gamma_{jk}^{(1)}$ is one of the eigenvalues of the coefficient matrix of the linear system defined by Eq. (6), which we discussed earlier.

If we assume the special case when $N=3$, $m=2$, $p=1$, $\mathbf{g}(\mathbf{u}_{j,n})=\mathbf{0}$, and $\mathbf{z}_0=\mathbf{0}$ in Eq. (5), then we have

$$\begin{cases} z_{j,n+1} = z_{jn} + \alpha_{jk}^{(1)}(z_{jn} - z_{kn}) + \alpha_{jk}^{(2)}(z_{jn} - z_{kn})^2 \\ \quad + \alpha_{jl}^{(1)}(z_{jn} - z_{ln}) + \alpha_{jl}^{(2)}(z_{jn} - z_{ln})^2, \\ z_{k,n+1} = z_{kn} + \alpha_{kl}^{(1)}(z_{kn} - z_{ln}) + \alpha_{kl}^{(2)}(z_{kn} - z_{ln})^2 \\ \quad + \alpha_{kj}^{(1)}(z_{kn} - z_{jn}) + \alpha_{kj}^{(2)}(z_{kn} - z_{jn})^2, \\ z_{l,n+1} = z_{ln} + \alpha_{lj}^{(1)}(z_{ln} - z_{jn}) + \alpha_{lj}^{(2)}(z_{ln} - z_{jn})^2 \\ \quad + \alpha_{lk}^{(1)}(z_{ln} - z_{kn}) + \alpha_{lk}^{(2)}(z_{ln} - z_{kn})^2, \end{cases} \quad (15)$$

We will see in a companion paper to appear soon that even a quadratic system which is a special case of our general model described by Eq. (5) exhibits excitingly richer dynamical properties in its solution curve than linear systems.

4. Classification of the dynamical scenarios of the linear systems

4.1 Dyadic cases

In this subsection, we discuss the dynamical scenarios of the linear systems described by Eq. (7). As pointed out earlier, dynamical scenarios of the solution curves of these systems have three patterns depending on the absolute value of one of the eigenvalues, $1 + \alpha_{jk} + \alpha_{kj}$, the other eigenvalue being 1.

Simulation 1, Case 1 is the case when both eigenvalues are 1 (i.e., a double root). In this case, two members diverge to infinity on the parallel lines preserving their distance in the complex plane (Figure 6).

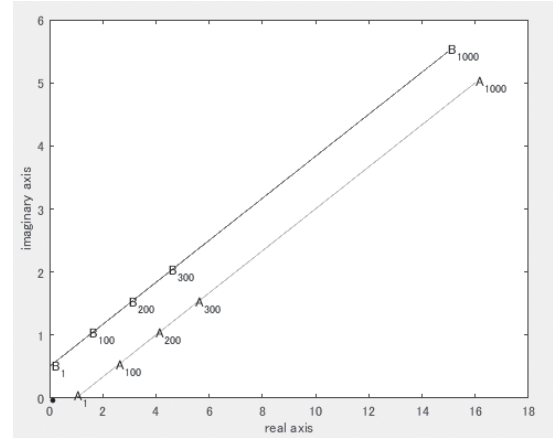


Fig. 6. Trajectories of two members j ($=A$) and k ($=B$) on the complex plane in the special case when $\alpha_{jk} = 0.01(1+i)$, $\alpha_{kj} = -0.01(1+i)$.

It is interesting to notice that the angle between the two members converges asymptotically to zero as time pro-

ceeds. This means that the skewness of the similarity of the two members monotonically decreases preserving their distance as time proceeds. Such a relation might be reminiscent of that of a husband and wife who have lived together for a long time.

Simulation 1, Case 2 is the case when the absolute value of one eigenvalue is less than 1. In this case, two members converge to a fixed point in the complex plane (Figure 7). This point coincides with the asymptotic point of the trajectories which is solved algebraically by the Patzer algorithm.

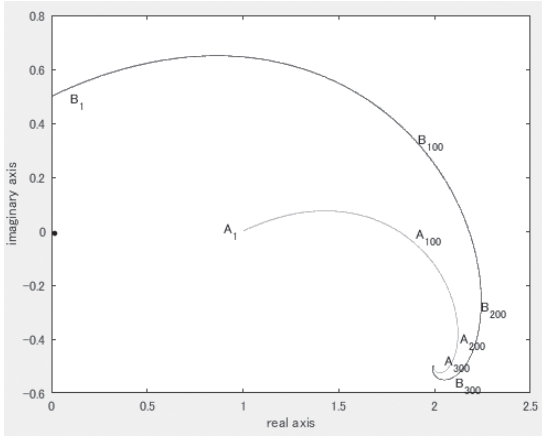


Fig. 7. Trajectories of two members $j (=A)$ and $k (=B)$ on the complex plane in the special case when $\alpha_{jk} = 0.01(1 + i)$, $\alpha_{kj} = -0.02(1 + i)$.

Simulation 1, Case 3 is the case when the absolute value of one eigenvalue is greater than 1. In this case, two members diverge to infinity in the complex plane (Figure 8).

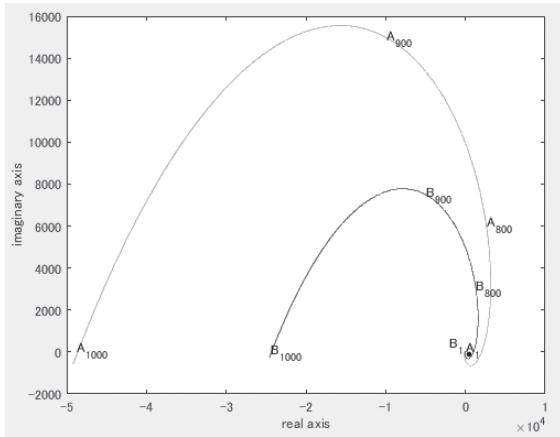


Fig. 8. Trajectories of two members $j (=A)$ and $k (=B)$ on the complex plane in the special case when $\alpha_{jk} = 0.02(1 + i)$, $\alpha_{kj} = -0.01(1 + i)$.

4.2 Triadic cases

In this subsection, we discuss the dynamical scenarios of the linear system described by Eq. (8). In this case, the coefficient matrix which determines the dynamical scenarios of the solution curve of Eq. (8) is written as the matrix A_3 in Eq. (10). The eigenvalues of this matrix are rather complicated. Of course, one of the three eigenvalues is always 1. In this case, the two eigenvalues except 1 determine the type of the dynamical scenario of this system. These two eigenvalues are written in the form, $1 + \frac{1}{2}\sum \alpha_{gh} \pm \frac{1}{2}\sqrt{D}$, where D is a function of α_{gh} . We shall show some patterns of the dynamical scenario of this system below.

Simulation 2, Case 1 (tripartite deadlock) is the case when the absolute values of two eigenvalues are greater than 1, and they are the same. In this case, the initial configuration of members can be said to be in the *tripartite deadlock* from the viewpoint of HFM. Members diverge to infinity preserving the state of tripartite deadlock as time proceeds (Figure 9). The direction of rotation of the trajectories in the plane is *counterclockwise*. If we change the coefficients α_{gh} a bit, we have trajectories whose direction of rotation is *clockwise*.

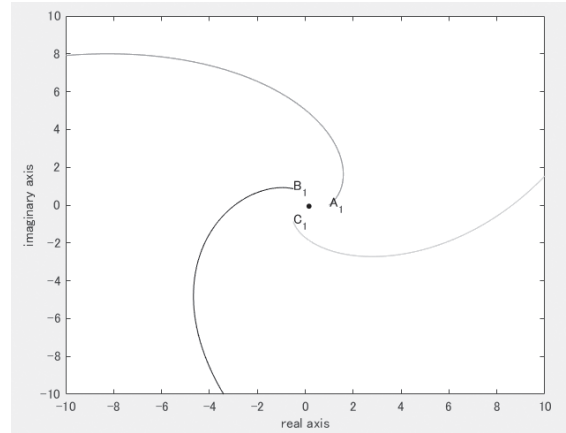


Fig. 9. Trajectories of two members $j (=A)$, $k (=B)$, and $l (=C)$ on the complex plane in the special case when $\alpha_{jk} = \alpha_{kj} = \alpha_{jl} = \alpha_{lj} = \alpha_{kl} = \alpha_{lk} = 0.01(1 + i)$.

Simulation 2, Case 2 (tripartite deadlock) is the case when the absolute values of two eigenvalues are both 1, i.e., a double root, while the other eigenvalue is less than 1. In this case, although the initial configuration of members is in the tripartite deadlock, it dissolves in a dyadic relation, as time proceeds (Figure 10).

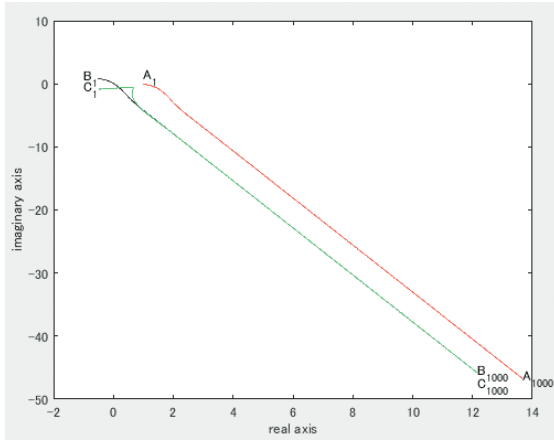


Fig. 10. Trajectories of two members $j (=A)$, $k (=B)$, and $l(=C)$ on the complex plane in the special case when $\alpha_{jk} = \alpha_{jl} = \alpha_{kl} = 0.01(1 - i)$, $\alpha_{kj} = \alpha_{lj} = \alpha_{lk} = -0.02(1 - i)$.

Simulation 2, Case 3 (tripartite deadlock) is the case when the absolute values of two eigenvalues are both less than 1. In this case, the initial tripartite deadlock state breaks down gradually and three members converge to a fixed point as time proceeds (Figure 11).

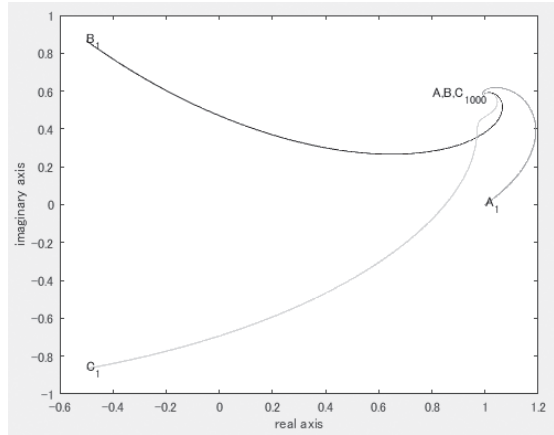


Fig. 11. Trajectories of two members $j (=A)$, $k (=B)$, and $l(=C)$ on the complex plane in the special case when $\alpha_{jk} = -0.01(1 - i)$, $\alpha_{jl} = \alpha_{kl} = 0.01(1 - i)$, $\alpha_{kj} = \alpha_{lj} = \alpha_{lk} = -0.02(1 - i)$.

Simulation 2, Case 4 (tripartite deadlock) is the case when the absolute values of two eigenvalues are both less than 1, as with Case 3. In this case, α_{jl} instead of α_{jk} was set to $-0.01(1 - i)$. As a result, the initial tripartite deadlock state breaks down gradually and three members converge to a fixed point as time proceeds, as in Case 3, but solution curves of the three members are different from those of Case 3 (Figure 12).

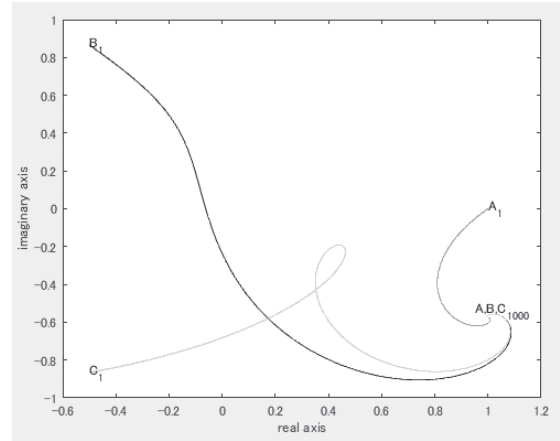


Fig. 12. Trajectories of two members $j (=A)$, $k (=B)$, and $l(=C)$ on the complex plane in the special case when $\alpha_{jk} = 0.01(1 - i)$, $\alpha_{jl} = -0.01(1 - i)$, $\alpha_{kl} = 0.01(1 - i)$, $\alpha_{kj} = \alpha_{lj} = \alpha_{lk} = -0.02(1 - i)$.

Simulation 2, Case 5 (tripartite deadlock) is the case when the absolute values of three eigenvalues are all ones, i.e., a *triple root*. In this case, the initial tripartite deadlock state breaks down gradually and three members diverge to infinity as time proceeds (Figure 13). Although trajectories of these members *look like straight lines at a glance*, algebraic solutions by the Patzer algorithm teach us that these trajectories are *quadratic curves*.

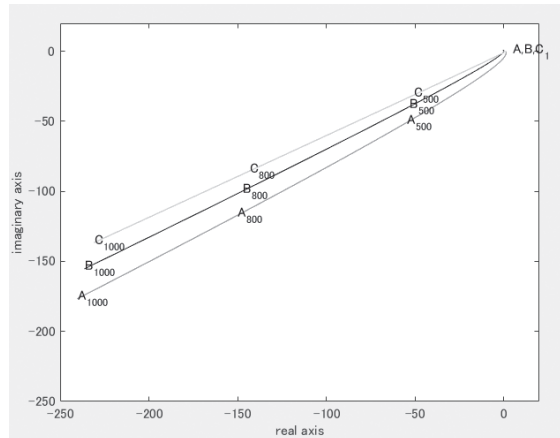


Fig. 13. Trajectories of two members $j (=A)$, $k (=B)$, and $l(=C)$ on the complex plane in the special case when $\alpha_{jk} = 0.01(1 - i)$, $\alpha_{jl} = 0.005(1 - i)$, $\alpha_{kl} = 0.01(1 - i)$, $\alpha_{kj} = -0.01(1 - i)$, $\alpha_{lj} = -0.005(1 - i)$, $\alpha_{lk} = -0.01(1 - i)$.

5. Classification of the dynamical scenarios of the linear systems with control term

In this section, we describe the dynamical scenario of a linear system with control term described by Eq. (5). In

general, such a system can be solved algebraically. For example, if we add a control term, $\mathbf{g}(\mathbf{u}_{j,n})$, to Eq. (9) which is a linear dyadic case, we have

$$\mathbf{z}_{n+1} = \mathbf{A}_2 \mathbf{z}_n + \mathbf{g}(\mathbf{u}_{j,n}). \quad (16)$$

Then, the solution curve can be written as

$$\mathbf{z}_n = \mathbf{A}_2^n \mathbf{z}_0 + \sum_{r=0}^{n-1} \mathbf{g}(\mathbf{u}_{j,r}) \quad (17)$$

where \mathbf{z}_0 is the initial coordinate vector.

In this case, we assume that the original dyadic linear system is the same as Simulation 1, Case2 discussed earlier, and $\mathbf{g}(\mathbf{u}_{j,n}) = ((0.01i)^n, (0.01(1+i))^n)^t$. In contrast to its solution curves, the solution curves of the system with a control term is shown in Figure 14.

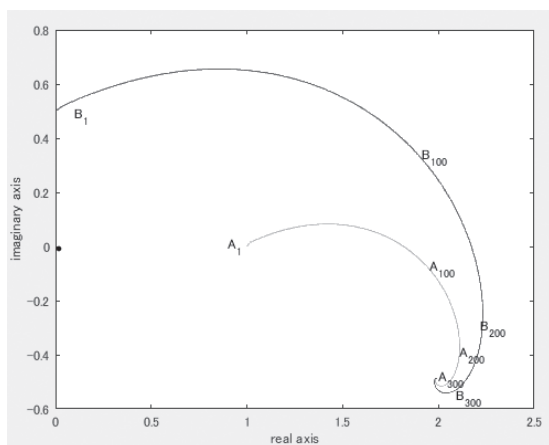


Fig. 14. Trajectories of two members j (=A) and k (=B) on the complex plane in the special case when $\alpha_{jk} = 0.01(1+i)$, $\alpha_{kj} = -0.02(1+i)$. In this case, a special control term is added to the original one.

6. Discussion

In this paper we have proposed a recent version of a set of complex difference equation models, which describes changes in asymmetric relationships among objects over time. Typical examples of these objects may be citation frequencies in scientific publications (i.e., Barabási & Albert, 1999; Chino, 1978), amounts of trade among nations (i.e., Chino, 1978), and connections among neurons (i.e., Aizenberg et al., 1971, 2000; Hirose, 1992; Suksmono & Hirose, 2005).

If we use the matrix notation, the above data at an instant of time is represented by a real asymmetric relational data matrix whose elements denote the magnitudes of proximity from object to object. Instead, if we utilize the graph theory, it is represented by a weighted directed graph (or abbreviated as digraph).

Let us now suppose that such an asymmetric relational data matrix (or a weighted digraph) is observed at an instant of time. Then, it is natural to ask the following questions. In what manner does the proximity among objects change theoretically as time proceeds, through the interactions among objects? How can we change the proximities among objects, or paraphrase it to say, how can we control these proximities?

To answer these questions, we apply the Chino-Shiraiwa theorem (Chino & Shiraiwa, 1993) to the asymmetric relational data matrix (or weighted digraph) observed at an instant of time, first. This theorem teaches us that objects which constitute the matrix are represented as points in a (complex) Hilbert space or in an indefinite metric space, depending on the definiteness of the matrix. However, we may embed objects in a complex plane (i.e., one-dimensional Hilbert space) if the largest eigenvalue of the Hermitian matrix computed from the real asymmetric relational data matrix observed at an instant of time is sufficiently large.

The difference equation model discussed in this paper considers these points embedded in the Hilbert space as initial points of the model and examines the possible theoretical scenarios of its trajectories utilizing the established theories and methods of difference equation as well as those of the complex dynamical system. In this sense our job might be said to be an introduction to an elementary theory of dynamic weighted digraph. In this paper, we have reported the part one of our theory, in which we have described a current difference equation model and have shown the possible theoretical scenarios of its trajectories of some special linear difference equation models. In a companion paper to be published soon, we shall discuss the possible theoretical scenarios of some nonlinear difference equation models, as a second part of our theory.

Acknowledgements

The author is indebted to Gregory L. Rohe for proofreading of an earlier version of this paper.

References

- Aihara, K., Ikeguchi, T., & Matsumoto, G. (1998). Deterministic nonlinear dynamics of a forced oscillation experimentally observed with a squid giant axon. *International Journal of Chaos Theory and its Applications*, *3*, 5-20.
- Aizenberg, N. N., Ivaskiv, Y. L., & Pospelov, D. A. (1971). A certain generalization of threshold functions. *Doklady Akademii Nauk SSSR*, *196*, 1287-1290.
- Aizenberg, I. N., Aizenberg, N. N., & Vandewalle, J. (2000). *Multi-valued and universal binary neurons—Theory, Learn-*

- ing and Applications*. Boston: Kluwer Academic Publishers.
- Babloyantz, A. & Destexhe, A. (1986). Low-dimensional chaos in an instance of epilepsy. *Proceedings of the National Academy of Sciences*, **83**, 3513-3517.
- Barabási, A-L. & Albert, R. (1999). Emergence of scaling in random networks. *Science*, **286**, 509-512.
- Chesson, P. L. & Warner, R. R. (1981). Environmental variability promotes coexistence in lottery competitive systems. *American Naturalist*, **117**, 923-943.
- Chino, N. (1978). A graphical technique for representing the asymmetric relationships between N objects. *Behavior-metrika*, **5**, 23-40.
- Chino, N. (2000). Complex differential system models of social interaction. *Bulletin of the Faculty of Letters of Aichi Gakuin University*, **30**, 43-54.
- Chino, N. (2016). A general non-Newtonian n-body problem and dynamical scenarios of solutions. *Paper presented at the 31th International Congress of Psychology*. Yokohama, Japan.
- Chino, N., & Shiraiwa, K. (1993). Geometrical structures of some non-distance models for asymmetric MDS. *Behavior-metrika*, **20**, 35-47.
- Dafillis, M. P., Frascoli, F., Cadusch, P. J., & Liley, D. T. J. (2013). Four dimensional Chaos and intermittency in a mesoscopic model of the electroencephalogram. *Chaos*, **23**, 230117-1-7.
- Elaydi, S. N. (1996). *An introduction of difference equations*. New York: Springer.
- Harary, F. (1969). *Graph theory*. Massachusetts: Addison-Wesley.
- Hirose, A. (1992). Continuous complex-valued back-propagation learning. *Electronics Letters*, **28**, 1854-1855.
- Korn, H., & Faure, P. (2003). Is there chaos in the brain? II. Experimental evidence and related models. *Comptes Rendus Biologies*, **326**, 787-840.
- Mandelbrot, B. B. (1977). *The fractal geometry of nature*. San Francisco: W. H. Freeman and Company.
- McCann, K., Hastings, A., & Huxel, G. R. (1998). Weak trophic interactions and the balance of nature. *Nature*, **395**, 794-798.
- Mees, A., Aihara, K., Adachi, M., Judd, K., Ikeguchi, T., & Matsumoto, G. (1992). Deterministic prediction and chaos in squid axon response. *Physics Letters A*, **169**, 41-45.
- Ott, E., Grebogi, C., & Yorke, J. A. (1990). Controlling chaos. *Physical Review Letters*, **64**, 1196-1199.
- Pereda, E., Gamundi, A., Rial, R., & González, J. (1998). Non-linear behavior of human EEG: fractal exponent versus correlation dimension in awake and sleep stages. *Neuroscience Letters*, **250**, 91-94.
- Putzer, E. J. (1966). Avoiding the Jordan canonical form in the discussion of linear systems with constant coefficients. *American Mathematical Monthly*, **73**, 2-7.
- Suksmono, A. B., & Hirose, A. (2005). Beamforming of ultra-wideband pulses by a complex-valued spatio-temporal multilayer neural network. *International Journal of Neural Systems*, **15**, 85-91.
- Takane, Y. (2015). Analysis of brain connectivity through fMRI data: Dynamic GSCA and GCANO. *Paper given as the Yanai Lecture at the 43th Meeting of the Behaviormetric Society of Japan*. September 3, Japan.
- Watts, D. J. & Strogatz, S. H. (1998). Collective dynamics of 'small-world' networks. *Nature*, **393**, 440-442.

(Final version submitted on September 29, 2017)